

Research Article

Biophysical and RNA Interference Inhibitory Properties of Oligonucleotides Carrying Tetrathiafulvalene Groups at Terminal Positions

Sónia Pérez-Rentero,¹ Alvaro Somoza,² Santiago Grijalvo,¹ Jiří Janoušek,³
Martin Bělohradský,³ Irena G. Stará,³ Ivo Starý,³ and Ramon Eritja¹

¹ Institute for Advanced Chemistry of Catalonia (IQAC), CSIC, CIBER-BBN Networking Centre on Bioengineering, Biomaterials and Nanomedicine, Jordi Girona 18-26, 08034 Barcelona, Spain

² IMDEA-Nanociencia, 28049 Madrid, Spain

³ Institute of Organic Chemistry and Biochemistry, v.v.i., Academy of Sciences of the Czech Republic, Flemingovo Náměstí 2, 16610 Prague 6, Czech Republic

Correspondence should be addressed to Ramon Eritja; recgma@cid.csic.es

Received 22 April 2013; Accepted 5 June 2013

Academic Editor: Rachid Benhida

Copyright © 2013 Sónia Pérez-Rentero et al. This is an open access article distributed under the Creative Commons Attribution License, which permits unrestricted use, distribution, and reproduction in any medium, provided the original work is properly cited.

Oligonucleotide conjugates carrying a single functionalized tetrathiafulvalene (TTF) unit linked through a threoninol molecule to the 3' or 5' ends were synthesized together with their complementary oligonucleotides carrying a TTF, pyrene, or pentafluorophenyl group. TTF-oligonucleotide conjugates formed duplexes with higher thermal stability than the corresponding unmodified oligonucleotides and pyrene- and pentafluorophenyl-modified oligonucleotides. TTF-modified oligonucleotides are able to bind to citrate-stabilized gold nanoparticles (AuNPs) and produce stable gold AuNPs functionalized with oligonucleotides. Finally, TTF-oligoribonucleotides have been synthesized to produce siRNA duplexes carrying TTF units. The presence of the TTF molecule is compatible with the RNA interference mechanism for gene inhibition.

1. Introduction

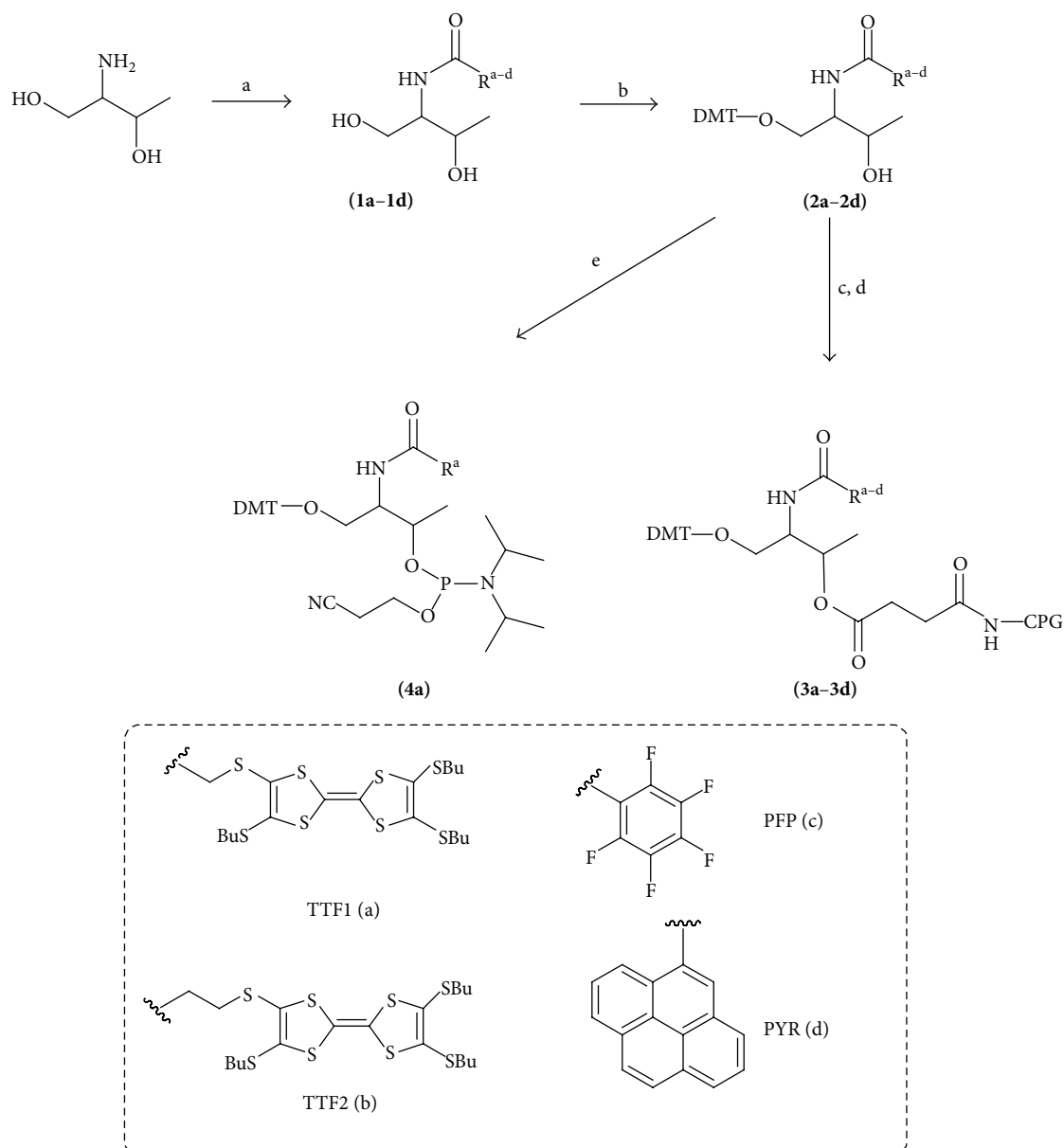
There is a current interest in the preparation of oligonucleotide conjugates with functional π -electron systems since their π - π interaction may provide additional binding energy without perturbing the specific recognition with the complementary sequences. Several authors have described aromatic systems that linked to the 3' end and 5' end of oligonucleotides inducing the stabilization of DNA duplexes by π - π stacking interactions [1–6].

Recently, we have reported that the introduction of tetrathiafulvalene (TTF) derivatives at the terminal position of oligonucleotides induces a high stabilization of the DNA duplexes. Moreover, depending on the location of the TTF molecules, a strong aggregation was observed at high salt concentrations yielding defined spherical nanostructures of around 190–210 nm of size [7]. TTF molecules are strong electron-donating molecules which have been used for the

construction of organic conducting materials [8] or as building blocks in supramolecular chemistry [9].

In this study, we aim to compare the duplex stabilization properties of TTF units paired with other donor or acceptor aromatic molecules. To this end, we synthesized several oligonucleotides carrying a TTF unit functionalized with three aliphatic *S*-butyl groups (Scheme 1) at either 3' or 5' ends of the oligonucleotide. Their complementary oligonucleotide sequences carrying TTF, pyrene, or pentafluorophenyl groups were used to form DNA duplexes with the donor/acceptor hydrophobic π -electron systems molecules at the same or opposite termini of the duplex. The relative thermal stability of the duplexes was analyzed demonstrating a distinct behavior of the TTF oligonucleotide conjugates that is in agreement with the supramolecular properties of TTF.

Moreover, there is an interest in the preparation of stable gold nanoparticles (AuNPs) functionalized with oligonucleotides. DNA oligomers carrying thiol and dithio groups



SCHEME 1: Preparation of the solids supports and phosphoramidite **4a** needed for the assembly of oligonucleotides. (a) R-COOH, EDCl, 1-hydroxybenzotriazole, and DIEA; (b) dimethoxytrityl chloride, DMAP; (c) succinic anhydride, DMAP; (d) hemisuccinate, NH₂-controlled pore glass (CPG), TBTU, triethylamine; (e) O-2-cyanoethyl-N,N-diisopropyl chlorophosphoramidite.

are frequently used to functionalize citrate-stabilized gold nanoparticles [10–12]. The presence of eight thioether functions in TTF units prompted us to investigate the use of TTF-oligonucleotides for the functionalization of gold nanoparticles. As expected, TTF-modified oligonucleotides are able to bind to citrate stabilized gold nanoparticles (AuNPs) producing stable AuNPs functionalized with oligonucleotides. Finally, TTF-oligoribonucleotides have been synthesized to produce siRNA duplexes carrying TTF units. Chemical modification of the 3' ends of siRNA is an active area of research aimed at increasing the stability of modified siRNA [13, 14] as well as stabilizing the interaction of siRNAs with the PAZ domain of RISC [15]. In this work, we demonstrate that the presence of the TTF molecule is compatible with the RNA

interference mechanism for gene inhibition, especially if the TTF unit is located at the 3' ends of the passenger strand.

2. Materials and Methods

2.1. General Information. All the standard phosphoramidites and reagents for DNA synthesis were purchased from Applied Biosystems and from Link Technologies. L-threoninol, and other chemicals were purchased from Sigma-Aldrich and Fluka. TTF1-threoninol and pyrenyl-threoninol derivatives were prepared as described [7, 15]. {[4',5,5'-Tris(butylsulfanyl)-2,2'-bi-1,3-dithiol-4-yl]sulfanyl} acetic acid was prepared as described previously [16]. Dry solvents were purchased from Sigma-Aldrich and Fluka and used as received.

NMR spectra were recorded at 25°C on Varian Gemini 300 MHz, Varian Mercury 400, or Varian Inova 500 MHz spectrometers using deuterated solvents (Unitat de RMN, Serveis científicotècnics de Barcelona). Tetramethylsilane (TMS) was used as an internal reference (0 ppm) for ^1H spectra recorded in CDCl_3 and the residual signal of the solvent (77.16 ppm) for ^{13}C -spectra. For CD_2Cl_2 (53.8 ppm) and CD_3OD (49.0 ppm), the residual signal of the solvent was used as a reference. The external reference for ^{19}F -spectra was CCl_3F (0 ppm). Chemical shifts are reported in part per million (ppm) in the δ scale, coupling constants in Hz and multiplicity as follows: s (singlet), d (doublet), t (triplet), q (quadruplet), m (multiplet), and br (broad signal). Matrix-assisted laser desorption/ionization time-of-flight (MALDI-TOF) mass spectra were recorded on a Voyager-DE-RP spectrometer (Applied Biosystems) in negative mode by using 2,4,6-trihydroxyacetophenone (THAP)/ammonium citrate (CA) (1:1) as matrix and additive resp.). Electrospray ionization mass spectra (ESI-MS) were recorded on a Micro-mass ZQ instrument with single quadrupole detector coupled to an HPLC and high-resolution (HR) ESI-MS on an Agilent 1100 LC/MS-TOF instrument (Servei d'Espectrometria de Masses, Universitat de Barcelona).

2.2. 3-[[4',5,5'-Tris(butylsulfanyl)-2,2'-bi-1,3-dithiol-4-yl]sulfanyl]propionic Acid. (2-Cyanoethyl)sulfanyl TTF derivative [17] (1.2 g, 2.2 mmol) was dissolved in anhydrous DMF (50 mL) and degassed. A solution of $\text{CsOH}\cdot\text{H}_2\text{O}$ (0.43 g, 2.58 mmol, and 1.17 equiv.) in anhydrous MeOH (5 mL) was added. After stirring the reaction mixture at room temperature for 30 min, a suspension of 3-bromopropionic acid (0.5 g, 3.3 mmol, and 1.5 equiv.) and freshly annealed K_2CO_3 (1.8 g, 13 mmol, and 5.9 equiv.) in anhydrous DMF (60 mL) was added. The reaction mixture was stirred at room temperature for 2 h. A solution of 1 M HCl (20 mL) was added, and the mixture was extracted with EtOAc (3×100 mL). The organic phase was washed with water (3×100 mL), dried over anhydrous MgSO_4 , and concentrated to dryness under reduced pressure. The crude residue was purified by chromatography on silica gel (chloroform-methanol 100:0 to 90:10). The pure compound was crystallized from dichloromethane and heptane providing red crystals (1.02 g, 81%). Melting point: 70–71°C. IR (CHCl_3): $\nu = 3512$ w, 3091 w, 2961 s, 2932 s, 2875 s, 2864 m, 2739 w, 2656 w, 2581 w, 1746 w, 1713 s, 1583 mbr, 1485 w, 1465 m, 1458 m, 1433 m, 1419 m, 1381 m, 1289 m, 1197 w, 1100 w, 916 w, 887 cm^{-1} . UV-Vis (CHCl_3): λ_{max} (log ϵ) = 264 (4.18), 334 nm (4.14). ^1H NMR, δ_{H} (500 MHz, CD_2Cl_2): 0.92 (t, $J = 7.4$ Hz, 9H), 1.44 (h, $J = 7.4$ Hz, 6H), 1.61 (m, 6H), 2.73 (t, $J = 6.8$ Hz, 2H), 2.83 (t, $J = 7.4$, 6H), and 3.05 (t, $J = 6.8$ Hz, 2H). ^{13}C NMR, δ_{C} (126 MHz, CD_2Cl_2): 13.91, 22.19, 31.29, 32.37, 34.63, 36.54, 125.69 (=C-SCH₂), 128.44 (=C-SBu), 175.00 (COOH), and (=CS₂ not detected). ESI MS: 571 ([M]⁻), 499 ([M-(C₃H₅O₂)]⁻). HR ESI MS calcd for C₂₁H₃₁O₂S₈ 571.0095, found 571.0093.

2.3. {[4',5,5'-Tris(butylsulfanyl)-2,2'-bi-1,3-dithiol-4-yl]sulfanyl}-N-[(2R,3R)-1,3-dihydroxybutan-2-yl]propanamide (1b). A solution of {[4',5,5'-tris (butylsulfanyl)-2,2'-bi-1,3-dithiol-4-yl]sulfanyl}propanoic acid (0.61 mmol), L-threoninol (0.61 mmol), 1-ethyl-3-(3-dimethylaminopropyl)carbodiimide (EDCI) (0.91 mmol), hydroxybenzotriazole (HOBt) (0.91 mmol), and diisopropylethylamine (0.91 mmol) in anhydrous DMF (10 mL) was prepared under argon. After stirring the reaction mixture at room temperature overnight, the mixture was concentrated to dryness under reduced pressure. The residue was dissolved in toluene and concentrated to dryness under reduced pressure (3x). The residue was dissolved in dichloromethane (100 mL), and the organic phase was washed with 10% aqueous NaHCO₃ (2 × 50 mL) and saturated aqueous NaCl (50 mL). The organic phase was dried and concentrated to dryness under reduced pressure. The resulting TTF2-threoninol derivative was used in the next step without further purification. The desired compound was obtained as orange oil (338 mg, 83%). TLC (ethyl acetate) $R_f = 0.22$. ^1H NMR, δ_{H} (400 MHz, CDCl_3): 6.38 (d, $J = 6.8$ Hz, 1H, and NH), 4.20 (qd, $J = 6.4$ and 1.6 Hz, 1H), 3.88–3.83 (m, 3H), 3.13 (t, $J = 6.8$ Hz, 2H), 2.87–2.81 (m, 6H), 2.60 (td, $J = 6.8$ Hz and 2.4 Hz, 2H), 1.66–1.59 (m, 6H), 1.49–1.40 (m, 6H), 1.23 (d, $J = 6.4$ Hz, 3H), and 0.93 (t, $J = 7.6$ Hz, 9H). ^{13}C NMR, δ_{C} (100 MHz, CDCl_3): 171.5 (CO), 130.7 (C), 128.1 (C), 127.9 (C), 125.5 (C), 111.4 (C), 109.4 (C), 69.2 (CH), 65.3 (CH₂), 55.0 (CH), 36.9 (CH₂), 36.3 (CH₂), 36.2 (CH₂), 32.3 (CH₂), 32.0 (CH₂), 21.9 (CH₂), 21.8 (CH₂), 20.8 (CH₃), and 13.8 (CH₃). HRMS (ESI⁺): m/z : calc for C₂₅H₄₁NO₃S₈ ([M+H]⁺) 660.0930, found 660.0925.

2.4. N-[(2R,3R)-1,3-Dihydroxybutan-2-yl]-pentafluorobenzamide (1c). To a solution of pentafluorobenzoic acid (1.1 mmol) in DMF (2 mL) at room temperature, N-hydroxybenzotriazole (1.02 mmol) and diisopropylcarbodiimide (1.02 mmol) were added. After stirring the mixture for 5 min, L-threoninol (0.93 mmol) was added. The mixture was stirred at room temperature for 24 h and then quenched with methanol. The solvent was evaporated under vacuum, and the residue was purified by flash chromatography (cyclohexane-CH₂Cl₂-MeOH 6:3:0.5). The desired compound was isolated as a white solid (184 mg, 66%). ^1H NMR, δ_{H} (400 MHz, CD_3OD): 4.10 (dq, $J = 6.4$ and 2.7 Hz, 1H), 4.03 (dt, $J = 6.3$ and 2.7 Hz, 1H), 3.70 (system ABX, $J_{\text{AB}} = 10.9$ Hz, $J_{\text{AX}} = 6.5$ Hz, and $J_{\text{BX}} = 6.2$ Hz, 2H), 3.30 (m, 1H), and 1.22 (d, $J = 6.4$ Hz, 3H). ^{13}C NMR, δ_{C} (100 MHz, CDCl_3): 158.1 (C), 126.9 (C), 126.7 (C), 116.6 (C), 111.4 (C), 69.1 (CH), 64.9 (CH₂), 54.9 (CH), and 20.4 (CH₃). ^{19}F NMR, δ_{F} (376 MHz, CD_3OD): and -144.02 (d, $J = 19.2$ Hz, 2F), -156.3 (t, $J = 19.9$ Hz, 1F), -164.6 (m, 2F). HRMS (ESI⁺): m/z : calc for C₁₁H₁₁NO₃F₅ ([M+H]⁺) 300.0653, found 300.0660.

2.5. N-[(2R,3R)-1-(Bis(4-methoxyphenyl)(phenyl)methoxy)-3-hydroxybutan-2-yl]-[4',5,5'-tris(butylsulfanyl)-2,2'-bi-1,3-dithiol-4-yl]sulfanyl]propanamide (2b). The compound 1b (0.45 mmol) was dried by evaporation of anhydrous acetonitrile (ACN) under reduced pressure. The product was dissolved in anhydrous pyridine (5 mL), and reacted with 4,4'-dimethoxytriphenylmethyl chloride (0.68 mmol), diisopropyl ethylamine (1.02 mmol) and 4-dimethylaminopyridine (0.06 mmol, DMAP). After stirring for 6 h at room

temperature, 4,4'-dimethoxytritylchloride (0.68 mmol), and DMAP (0.06 mmol) dissolved in dry pyridine (5 mL) were added and the mixture was stirred at room temperature overnight. The reaction was quenched with methanol (0.5 mL) and the solvents were removed under reduced pressure. The residue was dissolved in toluene (3×10 mL) and evaporated to dryness. Then, the resulting material was dissolved in dichloromethane (100 mL), and the organic phase was washed with 5% aqueous NaHCO_3 (50 mL) and with saturated aqueous NaCl (50 mL). The solvent was evaporated and the residue was purified by chromatography on neutral aluminium oxide. The product was eluted with a slow gradient of ethyl acetate from 50 to 100% in hexane and then from 0 to 10% of methanol in ethyl acetate. The pure compound was obtained as an orange solid (226 mg, 55%). TLC (aluminium oxide) (ethyl acetate-hexane 2:1) $R_f = 0.54$. ^1H NMR, δ_{H} (400 MHz, CDCl_3): 7.40–6.82 (m, 13H), 6.20 (d, $J = 8.8$ Hz, 1H, NH), 4.09 (qd, $J = 6.4$ and 2.0 Hz, 1H), 3.97–3.92 (m, 1H), 3.79 (s, 6H), 3.42 (dd, $J = 9.6$ and 4.4 Hz, 1H), 3.30 (dd, $J = 9.6$ and 3.4 Hz, 1H), 3.10 (t, $J = 6.8$ Hz, 2H), 2.83–2.78 (m, 6H), 2.56 (t, $J = 6.8$ Hz, 2H), 1.65–1.56 (m, 6H), 1.47–1.38 (m, 6H), 1.15 (d, $J = 6.4$ Hz, 3H), 0.94–0.88 (m, 9H). ^{13}C NMR, δ_{C} (100 MHz, CDCl_3): 170.9 (CO), 158.8 (C), 144.5 (C), 135.7 (C), 135.5 (C), 130.7 (C), 130.2 (CH), 130.1 (CH), 128.3 (CH), 128.2 (CH), 128.1 (C), 128.0 (C), 127.3 (CH), 125.6 (C), 113.5 (CH), 113.4 (CH), 87.1 (C), 86.7 (CH), 65.3 (CH_2), 55.5 (CH_3), 53.8 (CH), 53.8 (CH), 37.0 (CH_2), 36.3 (CH_2), 36.2 (CH_2), 32.2 (CH_2), 32.0 (CH_2), 31.9 (CH_2), 21.9 (CH_2), 21.8 (CH_2), 20.2 (CH_3), 13.8 (CH_3). HRMS (ESI+): m/z : calc for $\text{C}_{46}\text{H}_{60}\text{NO}_5\text{S}_8$ ($[\text{M}+\text{H}]^+$) 962.2237, found 962.2065.

2.6. *N*-[(2*R*,3*R*)-1-(*Bis*(4-methoxyphenyl)(phenyl)methoxy)-3-hydroxybutan-2-yl]-pentafluorobenzamide (**2c**). To a solution of *N*-[(2*R*,3*R*)-1,3-dihydroxybutan-2-yl]-pentafluorobenzamide (0.53 mmol) in pyridine (2.6 mL) at 0°C, diisopropylethylamine (0.79 mmol), 4,4'-dimethoxytritylchloride (0.79 mmol) and 4-dimethylaminopyridine (0.1 mmol) were added. After 15 min the mixture was allowed to reach room temperature, then it was stirred for 24 h, and finally the reaction was quenched with methanol. The solvent was evaporated under vacuum, and the residue was purified by flash chromatography (cyclohexane-EtOAc 3:1). The desired compound was isolated as a yellowish solid (87 mg, 27%). ^1H NMR, δ_{H} (400 Mz, CDCl_3): 7.39 (d, $J = 7.2$ Hz, 1H), 7.29 (d, $J = 8.9$ Hz, 4H), 7.31–7.27 (m, 2H), 7.24–7.18 (m, 1H), 6.83 (d, $J = 8.9$ Hz, 4H) 6.69 (d, $J = 8.6$ Hz, 1H), 4.13 (d, $J = 5.4$ Hz, 1H), 4.15–4.10 (m, 1H), 3.79 (s, 6H), 3.49 (system *ABX*, $J_{\text{AB}} = 9.8$ Hz, $J_{\text{AX}} = 3.8$ Hz, and $J_{\text{BX}} = 3.3$ Hz, 2H), and 1.20 (d, $J = 6.4$ Hz, 3H). ^{13}C NMR, δ_{C} (100 Mz, CDCl_3): 158.7 (C), 157.6 (C), 144.1 (C), 135.3 (C), 135.0 (C), 129.9 (CH), 129.8 (CH), 129.1 (C), 128.1 (CH), 127.7 (CH), 127.1 (CH), 115.9 (C), 114.7 (C), 113.3 (CH), 113.1 (CH), 87.0 (C), 68.5 (CH_2), 65.4 (CH), 55.2 (CH_3), 54.1 (CH), 19.8 (CH_3). ^{19}F NMR, δ_{F} (376 MHz, CDCl_3): –140.7 (m, 2F), –151.2 (t, $J = 20.7$ Hz, 1F), and –160.3 (m, 2F). HRMS (ESI+): m/z : calc for $\text{C}_{32}\text{H}_{28}\text{NO}_5\text{F}_5\text{Na}$ ($[\text{M} + \text{Na}]^+$) 624.1779, found 624.1784.

2.7. *Functionalization of CPG Solid Supports (3b-3c)*. The DMT derivatives (**2b-2c**) were reacted with succinic anhydride and then incorporated on a long-chain alkylamine-controlled pore glass support (LCAA-CPG) as follows. The DMT derivative (0.09 mmol) was dried by evaporation with anhydrous ACN under reduced pressure. The residue was dissolved in anhydrous pyridine (5 mL) under argon. Succinic anhydride (0.22 mmol) and DMAP (0.05 mmol) were dissolved in 1 mL of pyridine and added to the solution. After 4 h of stirring at room temperature, succinic anhydride (0.22 mmol) and DMAP (0.05 mmol) were dissolved in 1 mL of pyridine and added to the solution. The reaction mixture was allowed to react overnight. The solvent was removed under reduced pressure, and the residue was dissolved in toluene (3×10 mL) and evaporated to dryness. The resulting material was dissolved in dichloromethane (20 mL). The organic phase was washed twice with 10% NaHCO_3 (15 mL) and brine (15 mL), dried over MgSO_4 , and evaporated to dryness. The resulting monosuccinate derivative was used in the next step without further purification.

Amino-LCAA-CPG (CPG New Jersey, 73 μmol amino/g, 300 mg) was placed into a polypropylene syringe fitted with a polypropylene disc and washed sequentially with DMF, methanol, THF, DCM, and ACN (2×5 mL). Then, a solution of the appropriate homosuccinate (44 μmol) and triethylamine (175 μmol) in anhydrous ACN (0.5 mL) was prepared. The solution was added to the support, and then a solution of 2-(1*H*-benzotriazole-1-yl)-1,1,3,3-tetramethyluronium tetrafluoroborate (TBTU) (175 μmol) in anhydrous ACN (300 μL) was added. The mixture was left to react for 1 h. The support was washed with DMF, methanol, DCM, and ACN (2×5 mL). The degree of functionalization was determined by analysis of the DMT released upon the treatment of an aliquot of the support with a 3% solution of trichloroacetic acid in DCM. The coupling procedure was repeated once more if needed, and the functionality of the resin was determined by DMT quantification ($f = 32$ $\mu\text{mol/g}$ for **3b** and 50 $\mu\text{mol/g}$ for **3c**, DMT cation, $\lambda_{\text{max}} 498$ nm, $\epsilon = 71.700 \text{ M}^{-1} \text{ cm}^{-1}$). Finally, the solid support was treated with the mixture of $\text{Ac}_2\text{O}/\text{DMF}$ (1:1, 500 μL) to cap free amino groups.

2.8. *Oligonucleotide Synthesis (DNA)*. The unmodified oligonucleotide sequences **1** ($5'$ TAG AGG CTC CAT TGC $3'$), **2** ($5'$ GCA ATG GAG CCT CTA $3'$), and **8** ($5'$ CGC GAA TTC GCG $3'$) were synthesized on a DNA/RNA synthesizer (*Applied Biosystems 3400*) using 200 nmol scale LV200 polystyrene supports and commercially available chemicals. The benzoyl (Bz) group was used for the protection of the amino group of C and A and the isobutyryl (^tBu) group for the protection of G. The coupling yields were >97%. The last DMT group was removed at the end of the synthesis. Each solid support was treated with aqueous concentrated ammonia at 55°C for 12 h to cleave the products from the supports and remove the benzoyl and isobutyryl groups. The mixtures were filtered and ammonia solutions were evaporated to dryness. Unmodified oligonucleotides were desalted with *Sephadex G-25* (NAP-10 column) and analyzed by HPLC. Column: XBridge OST C_{18} (4.6×50 mm, 2.5 μm).

Solvent A: 5% ACN in 100 mM triethylammonium acetate (TEAA) (pH = 7) and solvent B: 70% ACN in 100 mM TEAA (pH = 7). Flow rate: 1 mL/min. Conditions: 10 min of linear gradient from 0 to 30% B at room temperature for oligonucleotides **1** and **2** and at 60°C for oligonucleotide **8**. The resulting oligomers were analyzed by mass spectrometry (MALDI-TOF) and UV/Vis spectroscopy and used without further purification.

Oligonucleotides **3** and **4** (^{5'}TAGAGGCTCCATTGC^{3'}-TTF1 and ^{5'}GCAATGGAGCCTCTA^{3'}-TTF1, resp.), containing the TTF1 modification at the 3' ends were synthesized on a 0.5 μmol scale using the solid support functionalized with the TTF1 derivative and the oligonucleotide sequence **5** (TTF1-^{5'}GCAATGGAGCCTCTA^{3'}), containing the modification at the 5' ends, was synthesized on a 200 nmol scale employing LV200 polystyrene supports using the TTF-1-phosphoramidite as described [7].

Oligonucleotides **6** and **7** (^{5'}TAGAGGCTCCATTGCX^{3'}) and **9** and **10** (^{5'}CGCGAATTCGCGX^{3'}), X being the pyrenyl (PYR), and the 2,3,4,5,6-pentafluorophenyl (PFP), respectively, were synthesized on a 1 μmol scale using the corresponding solid support functionalized with the appropriate threoninol derivative prepared as described [15]. The syntheses were carried out as described above removing the last DMT group at the end of the synthesis. In this case only a 0.2 μmol of each solid support was treated with aqueous concentrated ammonia at 55°C for 12 h. The resulting oligonucleotides were desalted with *Sephadex G-25* (NAP-10 column) and purified by HPLC. Column: XBridge OST C₁₈ semipreparative column (10 × 50 mm, 2.5 μm). Flow rate: 3 mL/min. Conditions: 10 min of linear gradient from 0 to 30% of B at room temperature for oligonucleotides **6** and **7** and at 60°C for oligonucleotides **9** and **10**. The pure fractions were combined and evaporated to dryness. The purified oligonucleotides were analyzed by HPLC. Column: XBridge OST C₁₈ (4.6 × 50 mm, 2.5 μm). Flow rate: 1 mL/min. Conditions: 10 min of linear gradient from 0 to 30% of B at room temperature for oligonucleotides **6** and **7** and at 60°C for oligonucleotides **9** and **10**. The resulting oligomers were analyzed by mass spectrometry (MALDI-TOF) and UV/Vis spectroscopy as well. The yields obtained ranged from 25 to 41%.

2.9. Oligoribonucleotide (RNA) Synthesis. The unmodified 21-nucleotide RNA sequences **11** (^{5'}aucugaagaaggagaaaaTT^{3'}), **12** (^{5'}uuuuucuccuucucagauTT^{3'}), **13** (^{5'}gcuacagagaaucugauTT^{3'}), and **14** (^{5'}aucgaguuucucuguagcTT^{3'}) were synthesized on a DNA/RNA synthesizer (*Applied Biosystems 3400*) using 200 nmol scale LV200 polystyrene supports, 2'-TBDMS phosphoramidites, thymidine phosphoramidites, and commercially available chemicals. Guanosine was protected with the dimethylaminomethylidene group, cytosine was protected with the acetyl group, and adenosine with the benzoyl group. The last DMT group was left at the end of the synthesis. Each solid support was treated with a mixture of aqueous concentrated ammonia and ethanol (3:1) at 55°C for 1 h to cleave the products from the supports and remove the base protecting groups. The mixtures were

filtered, and the solutions were evaporated to dryness. Then, a mixture of *N*-methylpyrrolidone (NMP, 461 μL), triethylamine (TEA, 232 μL), and triethylamine trihydrofluoride (TEA·3HF, 307 μL) was prepared, and each dried sample was treated with 250 μL of the mixture for 2 h 30 min. at 65°C. Once the samples reached room temperature, 1.75 mL of a Tris Buffer solution (Glen-Pak RNA Quenching Buffer) was added and the oligonucleotides were purified with cartridges, (Glen-Pak RNA cartridge purification), following the procedure described by the manufacturer. The deprotected oligonucleotides were desalted with *Sephadex G-25* (NAP-10 column) and analyzed by HPLC. Column: XBridge OST C₁₈ (4.6 × 50 mm, 2.5 μm). Flow rate: 1 mL/min. Conditions: 10 min of linear gradient from 0 to 30% of B. The resulting oligomers were analyzed by mass spectrometry (MALDI-TOF) and UV/Vis spectroscopy (data not shown) and used without further purification. The yields obtained after cartridge purification ranged from 29 to 40%.

Oligonucleotide sequences **15** (^{5'}aucugaagaaggagaaaaTT^{3'}-TTF2) and **16** (^{5'}uuuuucuccuucucagauTT^{3'}-TTF2) (passenger and guide resp.), containing the TTF2 modification at the 3' ends (**3b**) were synthesized on a 0.5 μmol scale using the solid support functionalized with the TTF2 derivative. The synthesis was carried out as described above removing the last DMT group. The cleavage and deprotection steps were performed as described above using 0.25 μmol of each solid support. The products were purified by HPLC on an XBridge OST C₁₈ semipreparative column (10 × 50 mm, 2.5 μm). Flow rate: 3 mL/min. Conditions: 3 min of linear gradient from 0 to 9% B, then 1 min of linear gradient from 9 to 60% B, then 16 min of linear gradient from 60 to 75% B. The purified oligomers were analyzed by mass spectrometry (MALDI-TOF), UV/Vis, and HPLC. Column: XBridge OST C₁₈ (4.6 × 50 mm, 2.5 μm) using the conditions described above except the flow rate that was 1 mL/min. The yields obtained after HPLC purification ranged from 5 to 8%.

2.10. Melting Experiments Performed with Nonself-Complementary Oligonucleotides. The melting experiments were performed in duplicate at 3.3 μM of duplex concentration. The solutions were prepared either in 50 mM or in 1 M NaCl and 10 mM sodium phosphate buffer (pH = 7). The samples were heated at 90°C for 5 min, allowed to cool slowly to room temperature to induce annealing and then kept overnight in a refrigerator at 4°C. Melting curves were recorded by heating the samples with a temperature controller from 15 to 80°C or from 15 to 95°C at a constant rate of 1°C/min by measuring the absorbance at 260 nm. When the temperature was below 25°C, argon was flushed to prevent water condensation on the cuvettes. The absorption spectra and melting experiments (absorbance versus temperature) were recorded in 1 cm path-length cells. The *T_m* values were calculated with the *Meltwin 3.2* software.

2.11. Melting Experiments on Self-Complementary Oligonucleotides. The melting experiments were performed in duplicate at 6.6 μM oligonucleotide concentration as described above. Melting curves were recorded by heating the samples

with a temperature controller from 15 to 95°C at a constant rate of 1°C/min by monitoring the absorbance at 260 nm.

2.12. Preparation of Oligonucleotide Gold Nanoparticle Conjugates. Citrate stabilized gold nanoparticles (9.7 nm) were purchased from BBI Life Sciences and used as received. To prepare the conjugates, 5 nmol of tetrathiafulvalene modified oligonucleotide (**3** or **4**) dissolved in 1 mL of water was added to 1 mL of the gold nanoparticle solution (9.4 nM). The mixture was shaken for 16–20 h prior to salt stabilization. Then, the solution was brought to a final concentration of 10 mM sodium phosphate (pH = 7.2). The mixture was then allowed to equilibrate for 30 min before bringing the concentration to 0.15 M NaCl over a 7 h 30 min period in a stepwise manner (0.05 M NaCl increments each 2 h 30 min). The solutions were sonicated for 20 s before each addition to keep the particles dispersed during the salting procedure. The salting process was followed by incubation overnight at room temperature. Finally, to remove all unbound oligonucleotides, the solution was centrifuged at 13,200 rpm for 30 min. The supernatant was removed, and the reddish solid at the bottom of the centrifuge tube was dispersed in 1 mL of a 0.15 M NaCl, 10 mM sodium phosphate buffer (pH = 7.2). This procedure was repeated three times. The resulting conjugates were resuspended in 1 mL of a 0.15 M NaCl, 10 mM sodium phosphate (pH = 7.2), and 0.1% NaN₃ solution. Then, each solution was analyzed by UV-visible absorption spectroscopy, (**3**-AuNP: 7.43 nM and **4**-AuNP: 7.75 nM). The extinction coefficient used was the same as that used for unmodified nanoparticles ($\epsilon_{520} = 7.6 \times 10^7 \text{ M}^{-1} \text{ cm}^{-1}$, data provided by the manufacturer). Each solution was then stored in the fridge (4°C) prior to use.

2.13. Melting Experiments with Oligonucleotide-Gold Nanoparticle Conjugates. Melting experiments were performed in duplicate at 3.7 nM of each oligonucleotide gold-nanoparticle conjugate by mixing 498 μL of **3**-AuNP, 477 μL of **4**-AuNP, and 25 μL of the 0.15 M NaCl and 10 mM sodium phosphate buffer. The samples were heated at 90°C for 5 min, allowed to cool slowly to room temperature to induce annealing and then kept in a refrigerator at 4°C for 48 h. The solutions were sonicated for 20 s before the melting experiment to keep the particles dispersed. Melting curves were recorded by heating the samples with a temperature controller from 15 to 95°C at a constant rate of 1°C/min and when monitoring the absorbance at 523 nm. During the experiment, when the temperature was below 25°C, argon was flushed to prevent water condensation on the cuvettes. T_m values were determined from the maxima or the minima of the first derivative of the curves, calculated with the Origin 8.0 software.

2.14. Cell Culture. HeLa cells were grown at 37°C in Dulbecco's modified Eagle's medium (DMEM, GIBCO) supplemented with 10% fetal bovine serum (FBS) in a humidified atmosphere consisting of 5% CO₂ and 95% air. Cells were regularly passaged to maintain exponential growth. A day before transfection, at 50–80% confluency, cells were trypsinized and diluted with fresh medium ($\sim 1 \times 10^5$ cells/mL) and

transferred to 24-well plates (1 mL/plate). Four hours before transfection the medium was removed, and 500 μL of fresh medium was added. Two luciferase plasmids, firefly luciferase (pGL3) and *Renilla* luciferase (pRL-TK) from Promega, were used as control and reporter, respectively. For annealing of siRNAs, 0.2 μM of each strand was incubated using a 100 mM potassium acetate, 30 mM HEPES-KOH, and 2 mM magnesium acetate buffer (pH = 7.4). The samples were heated at 90°C for 1 min, allowed to cool slowly to room temperature to induce annealing and then kept at 37°C for 1 hour. Cotransfection of plasmids and siRNAs was carried out with Lipofectamine 2000 (Life Technologies) as described by the manufacturer for adherent cell lines. Then, 100 μL containing the plasmids (1.0 μg pGL3, 0.1 μg pRL-TK) and the corresponding siRNAs (1.8 nM) formulated into liposomes were applied per well. The final concentration of siRNAs per well was 0.3 nM. The cells were harvested 20 hours after transfection and lysed using passive lysis buffer (100 μL per well) according to the instructions of the Dual-Luciferase Reporter Assay System (Promega). The luciferase activities of the samples were measured using a MicroLuma Plus LB 96V Luminometer (Berthold Technologies) with a delay time of 2 s and an integrate time of 10 s. The following volumes were used: 20 μL of sample and 30 μL of each reagent (Luciferase Assay Reagent II and Stop and Glo Reagent). Ratios of target to control luciferase were normalized to a buffer control. The inhibitory effects generated by siRNAs duplexes were expressed as normalized ratios between the activities of the reporter *Renilla reniformis* (RL) and the control *Photinus pyralis* GL3 (pGL3) luciferase. The plotted data were averaged from three independent experiments \pm s.d.

3. Results and Discussion

3.1. Synthesis of End-Capped Oligonucleotides. L-threoninol was selected as a linker to incorporate TTF, pyrene or pentafluorophenyl moieties into DNA as illustrated in Scheme 1. Threoninol has been used as a linker to introduce TTF, pyrene, or pentafluorophenyl groups at the terminal positions essentially as described [7, 15, 18]. Two TTF molecules were used with a methylene of difference (Scheme 1). The synthesis of the threoninol derivative of the {[4',5,5'-tris (butylsulfanyl)-2,2'-bis-1,3-dithiol-4-yl]sulfanyl}acetic acid (TTF1, [16]) was described previously [7]. Using a similar protocol, the threoninol derivative of the {[4',5,5'-tris(butylsulfanyl)-2,2'-bis-1,3-dithiol-4-yl]sulfanyl}propionic acid (TTF2) was prepared in good yields. The threoninol derivative of the pentafluorophenyl (PFP) was prepared following the protocol described previously for the threoninol derivative of pyrene (PYR) [15].

Oligonucleotide (DNA and RNA) sequences **1–16** shown in Table 1 were prepared using a DNA/RNA synthesizer. For the synthesis of TTF-containing RNA molecules **15** and **16**, the TTF2 derivative was selected. As these oligonucleotides will be used in RNA interference experiments the extra methylene of the propionic acid derivative was judged to be potentially better in order to separate the TTF molecule from the RNA sequence as this may influence in the interaction with RISC [15]. Using standard protocols,

TABLE 1: Sequences of DNA and RNA oligonucleotides.

No.	Sequence (5'-3') ^(a)
1	TAG AGG CTC CAT TGC
2	GCA ATG GAG CCT CTA
3	TAG AGG CTC CAT TGC-TTF1
4	GCA ATG GAG CCT CTA-TTF1
5	TTF1-GCA ATG GAG CCT CTA
6	TAG AGG CTC CAT TGC-PYR
7	TAG AGG CTC CAT TGC-PFP
8	CGC GAA TTC GCG
9	CGC GAA TTC GCG-PYR
10	CGC GAA TTC GCG-PFP
11	auc uga aga agg aga aaa aTT
12	uuu uuc ucc uuc uuc aga uTT
13	gcu aca gag aaa ucu cga uTT
14	auc gag auu ucu cug uag cTT
15	auc uga aga agg aga aaa aTT-TTF2
16	uuu uuc ucc uuc uuc aga uTT-TTF2

^(a)TTF: tetrathiafulvalene, PYR: pyrene, PFP: 2,3,4,5,6-pentafluorophenyl. Base notation: DNA = A, C, and G; and T. RNA = a, g, c, and u.

the desired conjugates were obtained in good yields. The HPLC profiles and mass spectrometry data are shown as Supporting Information.

4. Melting Analysis

In a previous work, we described the effect of the TTF1 moiety linked to the 5' or 3' ends of oligonucleotides on the stability of the corresponding DNA duplexes [7]. Duplexes containing a TTF1 unit in each strand lead to either aggregation or strong duplex stabilization depending on the relative position of the TTF1 units and the concentration of salts. Here we aimed to study the effect of the presence of the TTF1 unit on the melting temperatures of duplexes carrying a π -donor group such as pyrenyl or a π -acceptor group like 2,3,4,5,6-pentafluorobenzyl. Results are summarized in Table 2. The T_m of the unmodified duplex (1 + 2) and duplexes containing a single TTF1 unit or two TTF1 units were included in the Table for comparison purposes. The melting experiments performed at 1 M NaCl are shown in Figure 1. Interestingly, no aggregation was observed under any conditions except for the duplex 3 + 4 carrying TTF units in opposite ends as described in reference [7]. Duplexes 6 + 2 and 7 + 2 carrying a single pyrenyl or 2,3,4,5,6-pentafluorobenzyl group showed a clear increase in stability as compared with 1 + 2 (ΔT_m ranging between 2.8 and 4.2). Such a change is higher than that observed at the TTF1 duplexes 1 + 4 and 3 + 2 (ΔT_m ranging between 0.8 and 2.8, Table 2). Therefore, the stabilization was slightly higher in the case of the pyrene-modified duplex 6 + 2 probably owing to an end-capping mechanism [1–6]. Duplexes 6+4 and 7+4 comprising both the TTF1 unit and the pyrenyl or 2,3,4,5,6-pentafluorobenzyl group at the opposite ends maintained the degree of stabilization (ΔT_m ranging between 4.9 and 5.4), which was found at the duplexes 6 + 2 and 7 + 2 containing the aromatic moieties alone. When the TTF1 unit and the pyrenyl or 2,3,4,5,6-pentafluorobenzyl












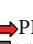


groups were placed at the same end of the duplexes 6 + 5 and 7 + 5, a similar stability was observed (ΔT_m ranging between 2.8 and 4.9) than in the previous case of 6 + 2 and 7 + 2 (ΔT_m ranging between 2.8 and 4.2). In the same conditions the duplex having two TTF1 units at the same end (3 + 4) had the highest increase on melting temperature (ΔT_m 10.9 and 18.8). This indicates the strong interaction between two TTF molecules.

In addition, we studied the effect on the thermal stability of the duplexes carrying two pyrenyl groups or two 2,3,4,5,6-pentafluorobenzyl groups placed at opposite ends of a duplex. To this end, we synthesized the unmodified self-complementary oligonucleotides 8 and the modified self-complementary oligonucleotides 9 (a pyrenyl group at the 3' ends) and 10 (a 2,3,4,5,6-pentafluorobenzyl group at the 3' ends). Results are summarized in Table 2. At low salt concentration (50 mM NaCl), a broad transition was observed that can be due to the presence of two transitions: the duplex to hairpin transition followed by the denaturation of the hairpin as described in a similar system [19] (Figure S5, C, see Supplementary Material available online at <http://dx.doi.org/10.1155/2013/650160>). At high salt concentration (1 M NaCl), a clear transition was observed. Previously, if TTF1 was present at the end of this sequence the formation of spherical aggregates was observed [7]. But now, with PYR and PFP groups, we did not observe the formation of any aggregate. So, the formation of aggregates is a particular property of oligonucleotides bearing TTF units.

When two PYR groups or two PFP groups were placed at opposite ends of the duplexes 9 + 9 and 10 + 10, we observed a clear increase in stability as compared with the nonmodified duplex ($\Delta T_m = 5.1$ for the duplex with two pyrenyl units and 3.5°C for the duplex containing two PFP units). Again we observed a higher stabilization in the case of the pyrene-modified duplex 9 + 9 probably owing to the aforementioned end-capping mechanism [1–6].

4.1. Gold Nanoparticle Functionalization with TTF1 Oligonucleotides. In addition, we studied the functionalization of gold nanoparticles with oligonucleotides containing the TTF1 modification. As oligonucleotides carrying thiol and dithio groups are used to functionalize citrate-stabilized gold nanoparticles [10–12], we consider that the presence of several thioether functions in TTF will be also useful for anchoring TTF-oligonucleotides onto the surface of gold nanoparticles. For this purpose oligonucleotides 3 and its complementary 4 carrying a TTF1 modification at the 3' ends were used. Immobilization of the modified oligonucleotides on 10 nm citrate-stabilized gold nanoparticles was carried out using previously described protocols that consists in the addition of the TTF-oligonucleotides to the AuNp suspension followed by slow increase of the salt concentration to reach 0.15 M NaCl [11]. The resulting material is then centrifuged, and the excess of TTF-oligonucleotide is washed out. The resulting functionalized gold nanoparticles were characterized by UV-vis spectroscopy (Figure 2(a)). After modification, only a small shift in the surface plasmon band was observed (from λ_{\max} 519 to 522 for 2-AuNp and from λ_{\max} 519 to 523 for 3-AuNp). The effect of the TTF1-modified oligonucleotides

TABLE 2: Melting temperatures of duplexes carrying pyrenyl (PYR), 2,3,4,5,6-pentafluorophenyl (PFP), or tetrathiafulvalene (TTF1) units.

Oligonucleotides	50 mM NaCl ^(a)	T_m (°C) (ΔT_m) ^(b)	1 M NaCl ^(a)	T_m (°C) (ΔT_m) ^(b)
1 + 2 	Duplex	55.8 (0)	Duplex	67.4 (0)
1 + 4 	Duplex	58.6 (2.8)	Duplex	69.5 (2.1)
3 + 2 	Duplex	57.2 (1.4)	Duplex	68.2 (0.8)
3 + 4 	Duplex	58.9 (3.1)	Aggregate	—
3 + 5 	Duplex	66.7 (10.9)	Duplex	86.2 (18.8)
6 + 2 	Duplex	60.0 (4.2)	Duplex	71.5 (4.1)
7 + 2 	Duplex	58.3 (3.0)	Duplex	70.2 (2.8)
6 + 4 	Duplex	60.9 (5.1)	Duplex	72.8 (5.4)
7 + 4 	Duplex	60.7 (4.9)	Duplex	72.6 (5.2)
6 + 5 	Duplex	60.2 (4.4)	Duplex	72.3 (4.9)
7 + 5 	Duplex	58.6 (2.8)	Duplex	71.0 (3.6)
8 	Duplex	Broad	Duplex	62.7 (0)
9 	Duplex	Broad	Duplex	67.8 (5.1)
10 	Duplex	Broad	Duplex	66.2 (3.5)

^(a)The shape of the UV spectra: “Duplex” indicates that a standard UV-vis spectrum of a duplex was observed and “Aggregate” indicates that a broad UV-vis spectrum with a large scattering was measured. ^(b) $\Delta T_m = T_m$ of a modified duplex minus T_m of an unmodified duplex under otherwise the same conditions. The arrows indicate the oligonucleotide orientation 5' \rightarrow 3'. Broad indicates a broad transition (supporting information, Figure S5).

on the stability of the conjugates was investigated following procedures described in the literature [20]. Each conjugate was treated with a DTT solution (10 mM) at 40°C and left to aggregate. Stability was evaluated by measuring the increment of absorbance at 675 nm that resulted from gold nanoparticle aggregation. The half-time $t_{1/2}$ (the time required to reach half the value for complete aggregation) was less than 1 min (data not shown), similar to other nanoparticles functionalized with disulfide bonds [20].

Moreover, we performed an hybridization assay with gold nanoparticles functionalized with complementary oligonucleotides. Assuming that the degree of gold nanoparticle functionalization was similar in each case, we prepared a 3.7 nM solution of each conjugate. The solution was incubated at 4°C for 48 h. The UV-vis spectrum was measured after annealing at 15°C. A plasmon band shift from 522/523 to 525 nm was observed, indicating that there is plasmonic interaction among the assembled AuNPs in the annealed solution. Then, a melting experiment at 523 nm was performed (Figure 2(b)). We observed a decrease in the absorbance with increasing temperature. We estimated the melting temperature as the midpoint of the curve ($\sim 61^\circ\text{C}$). The UV-vis spectrum was measured after the melting analysis at 85°C (Figure 2(a)). Comparing with the UV-vis spectrum recorded before annealing, we observed a small decrease in the absorbance and a shift of the plasmon band from 525 to 523 nm. This behaviour is different from gold nanoparticles

functionalized with thiol oligonucleotides that have larger changes in the visible spectra after hybridization [10–12], but it is in agreement with the small changes in the spectra observed with gold-nanoparticles organized by DNA origami [21]. For these reasons we believe that hybridization of gold nanoparticles with TTF-oligonucleotides induces a small number of contacts between AuNPs and for this reason the changes in the plasmon band are small. In any case, the stability of the DNA-TTF-functionalized gold nanoparticles is high as we do not observe changes in the aggregation state of the nanoparticles over the time.

4.2. Inhibition of the Luciferase Expression by siRNAs Modified with TTF2 Units. The presence of aromatic groups at the 3' ends of siRNAs has been previously investigated to stabilize the interactions between the 3' ends of siRNA and the hydrophobic pocket of the PAZ domain of RISC [15]. In addition, aromatic groups at the 3' end of siRNA efficiently protect siRNA from degradation of exonucleases present in the serum [15]. For these reasons we wanted to study the effect of the TTF modification at the 3' end of the siRNA. We selected the TTF2 modification at the 3' ends of the duplex siRNAs, and we analyzed the inhibition of the luciferase gene in HeLa cell line. As described before, the extra methylene of the propionic acid derivative was judged to be potentially better to separate the TTF molecule from the RNA sequence as this may influence in the interaction with RISC [15].

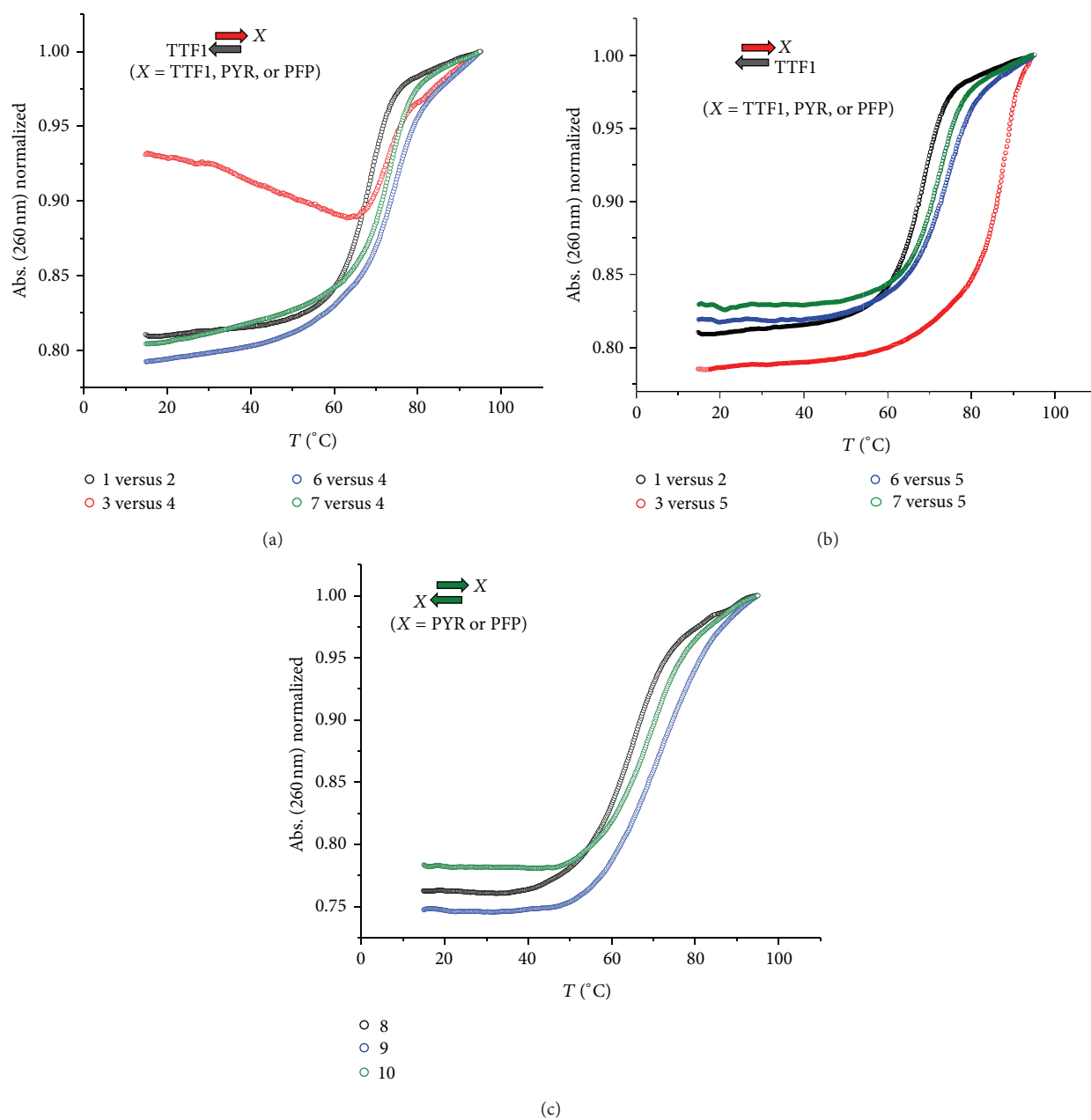


FIGURE 1: Melting curves of unmodified 15mer duplex **1 + 2** and duplexes carrying aromatic groups (a) at opposite sites and (b) at the same duplex site. (c) Melting curves of unmodified self-complementary duplex **8** and duplexes carrying two pyrene (**9**) or two pentafluorophenyl (**10**) units at opposite sites. Buffer: 1 M NaCl, 10 mM sodium phosphate buffer, pH = 7.

The duplexes used in this study were DUP1 (**12 + 15**, passenger strand modified with TTF2), DUP2 (**11 + 16**, guide strand modified with TTF2), and DUP 3 (**15 + 16**, both strands modified with TTF2). The siRNAs sequences were designed to inhibit *Renilla reniformis* luciferase. In addition, control experiments were performed with the unmodified duplex (WT, **11 + 12**) and with a scrambled siRNA (SCR, **14 + 15**). The *Renilla* luciferase inhibitory activity of modified siRNAs was evaluated using the dual-luciferase assay system after incubation with the corresponding siRNAs for 20 hours at 0.3 nM siRNA concentration. The inhibitory effects generated by siRNAs duplexes were expressed as normalized ratios

between the activities of the reporter *Renilla reniformis* (RL) and the control *Photinus pyralis* GL3 (pGL3) luciferase.

Figure 3 shows the amount of *Renilla* luciferase produced after 20 hrs of transfection with 0.3 nM unmodified siRNA (WT) or 0.3 nM of the same siRNA duplex carrying TTF2 at the 3' ends of passenger (DUP1) or guide strand (DUP2) or modified in both strands (DUP3). A scrambled siRNA duplex control sequence (Scr) was used as negative control. siRNA modified with TTF2 at the 3' ends of the passenger strand produced an inhibition of the production of *Renilla* luciferase of 60% compared to the negative controls that was less efficient than unmodified siRNA (75% inhibition). By contrast,

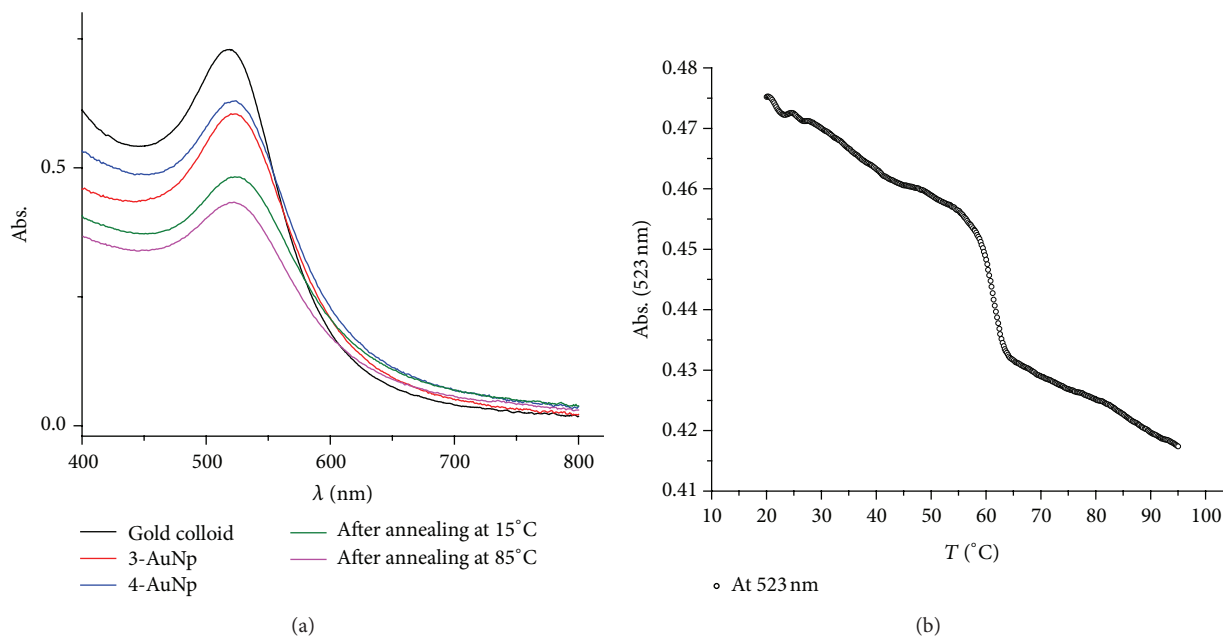


FIGURE 2: (a) UV-vis absorbance spectra of gold colloid (black), 3-AuNp, 4-AuNp conjugates (red and blue resp.) and 3-AuNp+4-AuNp after annealing measured at 15°C (green line) and at 85°C (pink line). (b) Melting curve of 3-AuNp+4-AuNp measured at 523 nm.

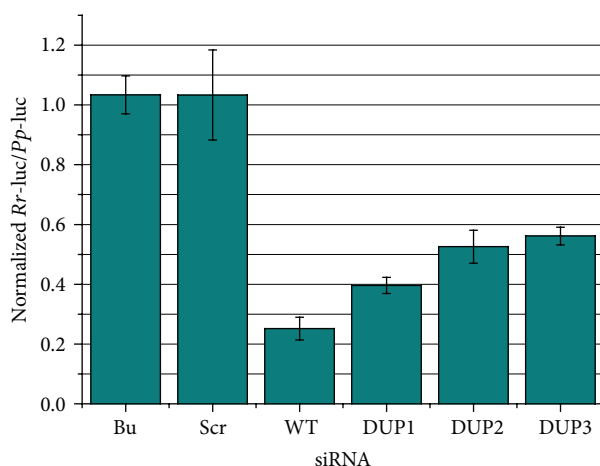


FIGURE 3: RNA interference activity of TTF2-modified siRNAs: DUP 1 (siRNA carrying a TTF2 unit at the 3'-end of passenger strand), DUP2 (siRNA carrying a TTF2 unit at the 3'-end of the guide strand) and DUP3 (siRNA carrying a TTF2 unit at both guide and passenger strands), WT (unmodified siRNA, wild type), Scr (scrambled siRNA), Bu: buffer alone. *Renilla reniformis* luciferase activity (*Rr-luc*) (target) versus *Photinus pyralis* pGL3 luciferase activity (*Pp-luc*) (control) after 20 hrs incubation of siRNA (0.3 nM) designed against *Renilla* gene in transiently transfected Hela cells. Ratios of target to control were normalized to a buffer control (Bu).

siRNAs containing TTF2 at the 3' ends of the guide strand or in both 3' ends of guide and passenger strands were clearly less efficient (52–57% inhibition). This result is in agreement with previous observations on other aromatic derivatives at the 3' ends of the guide strand in the inhibition of a luciferase gene [15]. In general, it can be concluded that the introduction of TTF at the 3' ends can be tolerated by the RNAi machinery

only if the passenger strand of an RNA duplex is functionalized. Although the results were not very promising, the hydrophobicity of the TTF derivatives can provide some extra advantage in the preparation of lipid formulations as it has been described by cholesterol-modified conjugates. Further work in this direction is needed to preclude the use of the TTF-modified siRNA in RNA interference.

5. Conclusions

In summary, we described the effect on the hybridization properties of 5'- or 3'-end-modified oligonucleotides with several planar aromatic compounds such as tetrathiafulvalene (TTF), pyrene (PYR), and pentafluorophenyl (PFP) groups. All these compounds induce the stabilization of DNA duplexes by end-capping mechanism as the PYR group the most stabilizing group followed by the PFP and being the TTF group the less stabilizing in duplexes carrying a single modification. In contrast when two TTF groups are located at the same terminus, the modified duplex is highly stabilized as a result of a strong π - π stacking interaction between the two TTF units. This interaction is less stable with the PYR:TTF pair and even less with the PFP:TTF pair. When two TTF groups are located at opposite ends, aggregate formation occurs, indicating interstrand π - π stacking interactions. This behaviour is only observed in duplexes carrying two TTF units. All these results show the strong π - π stacking interactions between TTF molecules in water, which are visualized by DNA duplex thermal denaturation experiments.

In addition, TTF-modified oligonucleotides are shown to be able to interact with gold nanoparticles producing stable oligonucleotide-TTF-gold nanoparticle conjugates. Finally, the synthesis and gene inhibitory properties of TTF-modified siRNAs are described for the first time, showing that the


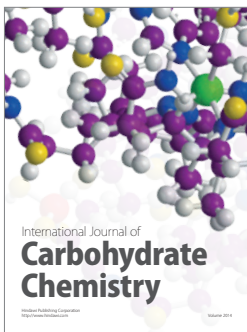
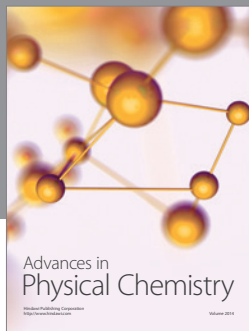
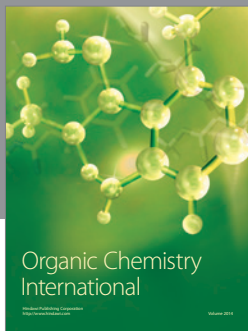
modification of the 3' ends of the passenger strand generates the most active siRNAs derivatives.

Acknowledgments

The authors thank Dr. Anna Aviñó for providing the non-modified oligonucleotides 11–14. This research was supported by the European Commission (Grants FP7-FUNMOL 213382 and NMP4-LA-2011-262943, MULTIFUN), by the Spanish Ministry of Education (grant CTQ2010-20541, SAF2010-15440), the Generalitat de Catalunya (2009/SGR/208), the Czech Science Foundation (P207/10/2214), the Ministry of Education, Youth and Sports of the Czech Republic (7E09054), and the Institute of Organic Chemistry and Biochemistry AS CR (RVO: 61388963). The authors declare no conflict of interests.

References

- [1] K. M. Guckian, B. A. Schweitzer, R. X.-F. Ren et al., "Experimental measurement of aromatic stacking affinities in the context of duplex DNA," *Journal of the American Chemical Society*, vol. 118, no. 34, pp. 8182–8183, 1996.
- [2] S. Narayanan, J. Gall, and C. Richert, "Clamping down on weak terminal base pairs: oligonucleotides with molecular caps as fidelity-enhancing elements at the 5'- and 3'-terminal residues," *Nucleic Acids Research*, vol. 32, no. 9, pp. 2901–2911, 2004.
- [3] Z. Dogan, R. Paulini, J. A. R. Stütz, S. Narayanan, and C. Richert, "5'-Tethered stilbene derivatives as fidelity- and affinity-enhancing molulators of DNA duplex stability," *Journal of the American Chemical Society*, vol. 126, no. 15, pp. 4762–4763, 2004.
- [4] S. Egetenmeyer and C. Richert, "A 5'-cap for DNA probes binding RNA target strands," *Chemistry*, vol. 17, no. 42, pp. 11813–11827, 2011.
- [5] A. Zahn and C. J. Leumann, "Recognition properties of donor- and acceptor-modified biphenyl-DNA," *Chemistry*, vol. 14, no. 4, pp. 1087–1094, 2008.
- [6] A. Aviñó, S. Mazzini, R. Ferreira, and R. Eritja, "Synthesis and structural properties of oligonucleotides covalently linked to acridine and quindoline derivatives through a threoninol linker," *Bioorganic and Medicinal Chemistry*, vol. 18, no. 21, pp. 7348–7356, 2010.
- [7] S. P. Pérez-Rentero, I. Gállego, A. Somoza et al., "Interstrand interactions on DNA duplexes modified by TTF units at the 3' or 5'-ends," *RSC Advances*, vol. 2, no. 10, pp. 4069–4071, 2012.
- [8] J. Yamada and T. Sugimoto, *TTF Chemistry, Fundamentals and Applications of Tetrathiafulvalene*, Springer, Berlin, Germany, 2004.
- [9] J. L. Segura and N. Martín, "New concepts in tetrathiafulvalene chemistry," *Angewandte Chemie*, no. 8, pp. 1372–1409, 2001.
- [10] S. J. Hurst, A. K. R. Lytton-Jean, and C. A. Mirkin, "Maximizing DNA loading on a range of gold nanoparticle sizes," *Analytical Chemistry*, vol. 78, no. 24, pp. 8313–8318, 2006.
- [11] Z. Li, R. Jin, C. A. Mirkin, and R. L. Letsinger, "Multiple thiol-anchor capped DNA-gold nanoparticle conjugates," *Nucleic Acids Research*, vol. 30, no. 7, pp. 1558–1562, 2002.
- [12] L. M. Demers, C. A. Mirkin, R. C. Mucic et al., "A fluorescence-based method for determining the surface coverage and hybridization efficiency of thiol-capped oligonucleotides bound to gold thin films and nanoparticles," *Analytical Chemistry*, vol. 72, no. 22, pp. 5535–5541, 2000.
- [13] J. K. Watts, G. F. Deleavey, and M. J. Damha, "Chemically modified siRNA: tools and applications," *Drug Discovery Today*, vol. 13, no. 19–20, pp. 842–855, 2008.
- [14] Y.-L. Chiu and T. M. Rana, "siRNA function in RNAi: a chemical modification analysis," *RNA*, vol. 9, no. 9, pp. 1034–1048, 2003.
- [15] Á. Somoza, M. Terrazas, and R. Eritja, "Modified siRNAs for the study of the PAZ domain," *Chemical Communications*, vol. 46, no. 24, pp. 4270–4272, 2010.
- [16] B.-T. Zhao, M.-J. Blesa, F. Le Derf et al., "Carboxylic acid derivatives of tetrathiafulvalene: key intermediates for the synthesis of redox-active calixarene-based anion receptors," *Tetrahedron*, vol. 63, no. 44, pp. 10768–10777, 2007.
- [17] H. Asanuma, K. Shirasuka, T. Takarada, H. Kashida, and M. Komiyama, "DNA-dye conjugates for controllable H* aggregation," *Journal of the American Chemical Society*, vol. 125, no. 8, pp. 2217–2223, 2003.
- [18] J. Rybáček, M. Rybáčková, M. Høj et al., "Tetrathiafulvalene-functionalized triptycenes: synthetic protocols and elucidation of intramolecular Coulomb repulsions in the oxidized species," *Tetrahedron*, vol. 63, no. 36, pp. 8840–8854, 2007.
- [19] A. Aviñó, S. Pérez-Rentero, A. V. Garibotti, M. A. Siddiqui, V. E. Márquez, and R. Eritja, "Synthesis and hybridization properties of modified oligodeoxynucleotides carrying non-natural bases," *Chemistry and Biodiversity*, vol. 6, no. 2, pp. 117–126, 2009.
- [20] S. P. Pérez-Rentero, S. Grijalvo, R. Ferreira, and R. Eritja, "Synthesis of oligonucleotides carrying thiol groups using a simple reagent derived from threoninol," *Molecules*, vol. 17, no. 9, pp. 10026–10045, 2012.
- [21] B. Ding, Z. Deng, H. Yan, S. Cabrini, R. N. Zuckermann, and J. Bokor, "Gold nanoparticle self-similar chain structure organized by DNA origami," *Journal of the American Chemical Society*, vol. 132, no. 10, pp. 3248–3249, 2010.



Hindawi

Submit your manuscripts at
<http://www.hindawi.com>

